An Image Synthesis Method Generating Underwater Images

Jarina Raihan Ahamed*, Pg Emeroylariffion Abas, Liyanage Chandratilak De Silva

Faculty of Integrated Technologies, Universiti Brunei Darussalam, Brunei Darussalam

Received 18 November 2021; received in revised form 23 January 2022; accepted 24 January 2022

DOI: https://doi.org/10.46604/aiti.2022.8938

Abstract

The objective of this study is to convert normal aerial images into underwater images based on attenuation values for different water types by utilizing the image formation model (IFM) with Jerlov water types. Firstly, the depth values are derived from RGB-D images. If the depth information is not available, the values between 0.5 m to 10 m are chosen, and the transmission map is estimated by these values. Secondly, the statistical average background light values of B_r = 0.6240, B_g = 0.805, and B_b = 0.7651 have been derived by analyzing 890 images using two methods, namely quad-tree decomposition and four-block division. Finally, the conversion of aerial-to-underwater images is done using the derived values, and the images are verified by computer simulation using MATLAB software. The result indicates that this method can easily generate underwater images from aerial images and makes it easier for the availability of ground truth.

Keywords: image processing, image synthesis, Jerlov water types, underwater image analysis

1. Introduction

Images that are captured underwater undergo distortions due to the optical properties of the water medium. Suspended particles and lighting conditions in the water distort the finally captured images due to the effect of absorption, scattering, diffraction, polarization, and so on. These reduce the visibility factor, brightness, sharpness, and edge information of underwater images, as well as increase their contrast and noise. Recently, image restoration and enhancement technologies have been increasingly used to restore underwater images and to recover useful information for various possible applications, such as seabed scene 3D reconstruction, target detection, classification of marine organisms, remotely operated vehicles [1], navigation and autonomous underwater vehicles (AUVs), etc. [2-3].

Image enhancement techniques, such as white balance, histogram equalization, and contrast stretching, may be used to recover the visibility, brightness, and contrast of images. However, degraded signal properties are not dealt with effectively by those techniques. Hence, there is a need to rely on the restoration process. Image restoration methods commonly rely on the underwater image formation model (IFM) to recover the degraded properties.

With the development of underwater image recovering techniques, the image quality evaluation of the restored underwater images is required to appraise the effectiveness of different restoration methods. Recently, non-reference metrics, i.e., underwater color image quality evaluation (UCIQE) [4] and underwater image quality measure (UIQM) [5], have been introduced as performance metrics specifically for underwater images. These measures focus on the hue, saturation, variance, and chroma of images. However, these non-reference metrics cannot properly analyze the signal properties but only give importance to the color properties of underwater images. An alternative is to use a full-reference image quality evaluation metric, which relies on a reference or a ground truth image. In normal foggy air images, popular full-reference image quality

* Corresponding author. E-mail address: jari3010@yahoo.in

evaluation metrics including peak signal-to-noise ratio (PSNR), structural similarity index (SSIM), and mean square error (MSE) may be used since ground truth images are easily obtainable. However, in an underwater scenario, it may be very difficult, if not impossible, to acquire a ground truth reference image for quality evaluation purposes. This makes it very challenging to use PSNR, SSIM, and MSE as evaluation tools to compare the restoration methods of underwater images.

An efficient dataset along with proper reference images is needed to evaluate different enhancement and restoration methods effectively. This study proposes a synthesis process for underwater images from aerial images. To create a publicly available dataset for underwater quality analysis, 890 aerial images are selected based on proper underwater image classification criteria and are then converted into underwater images. The synthesized underwater images are made based on Jerlov water types [6]. These synthesized images, with their corresponding original images functioning as reference images, may then be used to evaluate the performance of image enhancement and restoration methods.

The study is presented as follows. Section 2 reviews the studies related to image enhancement and restoration methods, particularly for underwater images. Section 3 presents the proposed synthesis method. Section 4 compares the evaluation results of the dataset using the proposed method and the methods selected from the literature. Finally, section 5 concludes the study.

2. Related Work: Underwater Enhancement, Restoration, and Synthesis Dataset

Image enhancement methods improve the visibility characteristics of underwater images, such as contrast, histogram, and color constancy. Hummel [7] proposed a basic enhancement approach by considering the histogram transformation of color channels. Subsequently, Zuiderveld [8] proposed an enhancement approach based on histogram equalization.

Iqbal et al. [9] proposed a two-fold method for enhancement, by first equalizing the color contrast and then adjusting the saturation of images. The same authors subsequently improve their proposed enhancement method, by using an enhanced unsupervised color-correction model (UCM) [10]. A histogram stretching approach has been proposed by Huang et al. [11] for shallow water image enhancement, whilst Ghani and Isa [12] have proposed a method to enhance underwater images through the composition of dual-intensity images and Rayleigh-stretching.

However, the enhancement methods primarily concentrate on the visibility of images, not on their structural and signal properties. On the other hand, the restoration methods of underwater images normally utilize the IFM as shown in Eq. (1) to restore the degraded signal properties.

$$I^c(x) = J^c(x).t^c(x) + (1 - t^c(x)).B^c; c \in \{R, G, B\} \tag{1}$$

In the above equation, $J^c(x).\, t^c(x)$ describes the radiance $J^c(x)$ of an object as it travels in the underwater medium, whilst $\left(1 - t^c(x)\right).\, B^c$ represents the scattering of background light B^c as it travels towards the camera. $I^c(x)$ is the observed image at the camera. The transmission map $t^c(x)$ describes the part of the object radiance that reaches the camera, after considering absorption and scattering. As such, it is dependent on the object's distance from the camera $d(x)$ (or its depth) and the water attenuation coefficient β^c in the color channel $c \in \{R, G, B\}$.

$$t^c(x) = e^{-\beta^c d(x)}; c \in \{R, G, B\} \tag{2}$$

From Eqs. (1) and (2), it can be seen that the radiance $J^c(x)$ of the object is attenuated exponentially with depth and water type. Recovering the original object radiance $J^c(x)$ from the acquired image $I^c(x)$ at the camera requires the knowledge of the background light B^c as well as the transmission map $t^c(x)$.

Raihan et al. [13] provided a detailed review of underwater image restoration methods, categorizing restoration methods into hardware and software approaches. Carlevaris-Bianco et al. [14] proposed a restoration method by estimating the depth of an underwater image. The depth estimation method is based on the strong attenuation prior difference among three color channels (i.e., red, green, and blue channels), considering the channels with maximum intensity prior. Dark channel prior (DCP) was initially introduced for the recovery of hazy images, but it has also been used for estimating both B^c and $t^c(x)$ for the underwater image restoration process [15]. The method relies on the assumption that dark pixels in an image are the pixels close to the camera as they get less brightening effect, whilst bright pixels are the pixels far away from the camera. Chao and Wang [16] proposed a method for the removal of scattering effects from water using DCP. The variation of DCP has also been proposed by considering green and blue channels only, neglecting the red channel [17]. Yang et al. [18] have also relied on the variation of DCP for the restoration of underwater images, by refining depth maps with a median filter instead of general soft matting.

Li et al. [19] proposed a blue-green channel restoration method by considering the extension of DCP and dehazing the red channel with gray-world assumption theory. Chiang and Chen [20] used DCP to estimate the transmission map and background light for underwater image restoration, using the fixed attenuation coefficient measured for the open ocean water. Peng and Cosman [21] proposed a method to restore the underwater images using a depth estimation process to develop the transmission map. Song et al. [22] proposed a restoration strategy based on the depth map estimation, involving the formation of a depth map based on the attenuation priors for each channel, which is then used to extract the background light and transmission map.

The literature points to the importance of image enhancement and restoration methods for different underwater applications. However, the performance comparison between different methods requires the presence of reference ground truth images, which may not be easily obtainable in difficult underwater conditions. Conversely, with the presence of the original image $J^c(x)$, underwater images may be synthesized using Eq. (1) to give $I^c(x)$. This needs to take into account the background light B^c and transmission map $t^c(x)$. The synthesized underwater images may then be fed into different enhancement and restoration methods with their restored output images used to compare against the original reference image $J^c(x)$, to derive different reference image quality evaluation metrics. These metrics shall then be used as a basis to compare the performance of different methods.

Numerous methods for synthesizing underwater images have been proposed in the literature. Zhao et al. [23] synthesized underwater images with depth values of 0.5 m to 3 m, which are a very short range for common underwater images. A fixed depth of 5 m has also been assumed and used to synthesize underwater images [17]. Anwar et al. [24] proposed a synthesizing method by considering depth values in the range of between 0.5 m and 15 m, which is a good range for a dataset with the ambient light set between 0.8 and 1.0 for all three color channels. However, ideally, the ambient light in all three channels should not be assumed to be identical. Liu and Chen [25] have chosen the ambient light based on a statistical ambient light estimating process as depicted in the work of He et al. [15], and have considered the depth values derived from the original depth maps from the selected dataset, for synthesizing the underwater images. However, the method used to estimate the ambient light may not be feasible in cases of underwater images, as it has been primarily designed for aerial images. Li et al. [26] have recently synthesized underwater images based on water types using the ambient light values ranging from 0.8 to 1.0 and the depth values between 0.5 m and 15 m. The method, however, lacks proper information on the ambient light as well as the depth value.

3. Proposed Method

Fig. 1 shows the flowchart of the proposed method, which is mainly governed by Eq. (1). Prior knowledge of water types, wavelengths, attenuation coefficients, depth, and background light is required in order to synthesize underwater images. Water types and wavelengths are used to determine the attenuation coefficient β^c, which is then used in the combination with the depth $d(x)$ to derive the transmission map $t^c(x)$ using Eq. (2). The original image $J^c(x)$, the background light B^c, and the derived transmission map $t^c(x)$ are then used to determine the synthesized image $I^c(x)$.

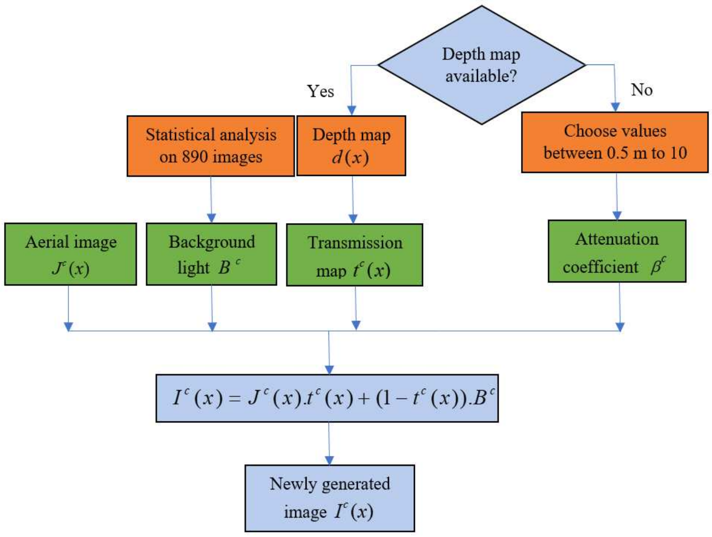

Fig. 1 Flowchart of the proposed method

Koczy and Jerlov [6] have analyzed the characteristics of seawater and have subsequently classified them into 10 types, based on different attenuation coefficients for different wavelengths of light in different seawater types. The attenuation coefficients play a vital role in underwater computer vision.

Fig. 2 shows the classification made based on each type's attenuation coefficient and wavelength. For more clarity, water types are classified broadly as oceanic and coastal waters. The oceanic water type includes type-I, type-IA, type-IB, type-II, and type-III subcategories, and the coastal water type includes type-1C, type-3C, type-5C, type-7C, and type-9C, from clear to turbid. Type-III and type-9C represent the most turbid in the oceanic water and coastal water categories, respectively. The attenuation coefficients for different water types are defined for the wavelength between 310 nm and 700 nm, which span the wavelength range of red, blue, and green lights underwater. Each type has its shades of blue and brown, which are shown in Fig. 3.

There is a total of 30 synthesized images generated using the proposed method with 3 ground truths and 3 ground truth depth maps. The synthesis dataset which is created by using the proposed method can be found using the link https://github.com/JarinaRaihan/UNDERWATER-SYNTHESIS-DATASET.

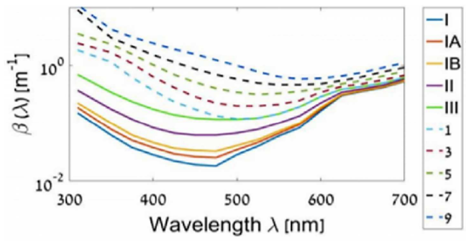

Fig. 2 Ten water types and their respective attenuation coefficients [24]

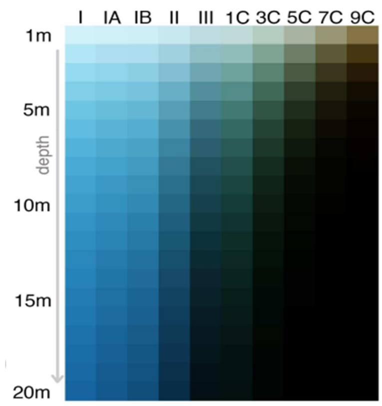

Fig. 3 Visual shades of the ten water types [27]

Solenko and Mobley [28] have selected the attenuation coefficients for each wavelength based on the inherent properties of water, chlorophyll concentration, diffusion, scattering, and absorption. The wavelengths for red, green, and blue channels are taken as 650 nm, 525 nm, and 475 nm, respectively. Based on the wavelengths, the attenuation coefficients are chosen and are given in Table 1. For the synthesis of underwater images, according to Eq. (1), $I^c(x)$ has to be synthesized using the given image $J^c(x)$ with the calculated transmission map $t^c(x)$ and background light B^c. To determine the transmission map $t^c(x)$, the attenuation coefficient β^c and depth map $d(x)$ are needed using Eq. (2). The obtained attenuation coefficient values β^c are shown in Table 1.

For a proper synthesis of underwater images, a ground truth depth map is of utmost importance. Hence, RGB-D images are chosen from a random dataset for synthesis. If the depth information is not available, the values from 0.5 m to 10 m may be chosen. The reason for this is that 5 types of water become dark and lose their color as the depth increases beyond 10 m. Unlike other synthesizing methods in the literature, the proposed method extracts the ambient light values by statistically evaluating the images based on two underwater ambient light estimation methods, which involve extracting the ambient light based on quad-tree decomposition and four-block division with the mean and standard deviation [21, 29]. Nearly 890 images have been analyzed, with the statistical average background or ambient light values of B_r = 0.6240, B_g = 0.805, and B_b = 0.7651.

Table 1 Attenuation coefficient values chosen based on Jerlov water types [6]

Water type	Red channel	Blue channel	Green channel
Type-I	0.85	0.96	0.98
Type-IA	0.84	0.95	0.97
Type-IB	0.83	0.95	0.96
Type-II	0.80	0.92	0.94
Type-III	0.75	0.88	0.89
Type-1C	0.75	0.88	0.87
Type-3C	0.71	0.82	0.80
Type-5C	0.67	0.73	0.67
Type-7C	0.62	0.61	0.50
Type-9C	0.55	0.46	0.29

4. Results and Discussion

This section discusses the results obtained from different restoration and enhancement methods for synthesized underwater images using the proposed method. State-of-the-art restoration and enhancement methods are selected from the literature to restore the synthesized underwater images. Their performance is appraised by conducting the quantitative and qualitative analysis of the restored underwater images.

Normal images are converted into underwater images based on Eq. (1), with the attenuation coefficient values chosen based on Table 1 for different water types. The original image (i.e., the ground truth image) and its corresponding ground truth depth map are given in Fig. 4(a) and Fig. 4(b), respectively. Fig. 5 depicts the resultant images for different Jerlov water types, which are synthesized from the original image in Fig. 4(a).

(a) Ground truth image

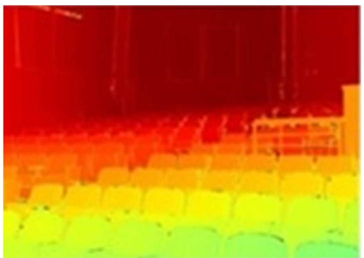

(b) Ground truth depth image

Fig. 4 Example of images from the dataset

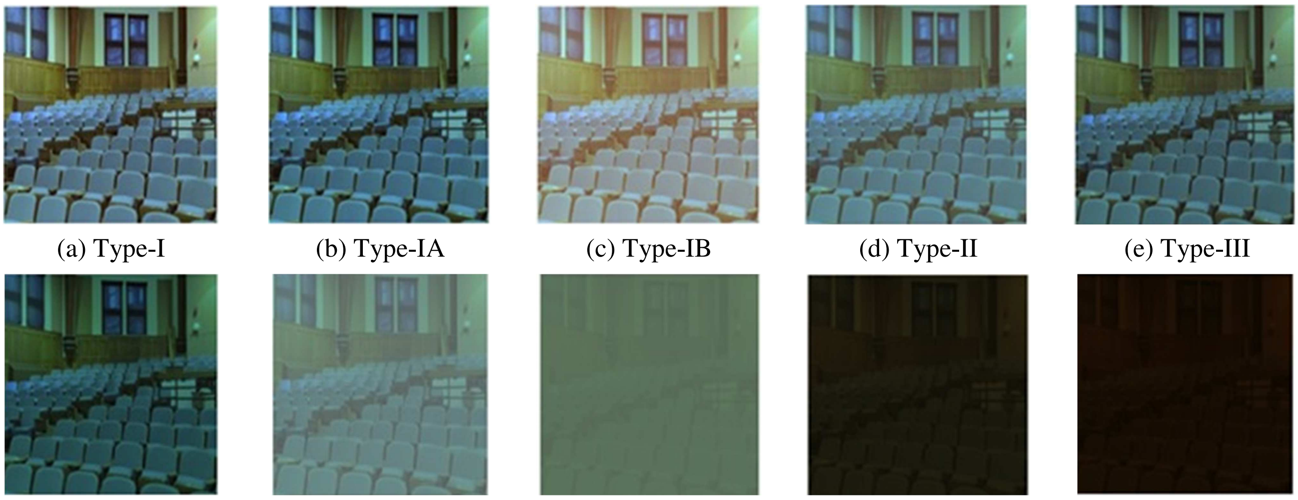

(a) Type-I (b) Type-IA (c) Type-IB (d) Type-II (e) Type-III

(f) Type-1C (g) Type-3C (h) Type-5C (i) Type-7C (j) Type-9C

Fig. 5 Synthesis of the underwater images showing Jerlov water types

The resultant images in Fig. 5 represent different underwater images for different water types. These representative underwater images are then processed using popular state-of-the-art restoration and enhancement methods in the literature, to give their corresponding restored images, which may then be compared to the ground truth image. Both qualitative and quantitative analyses are used. The qualitative analysis involves the evaluation of restored or enhanced images based on visual perception, whilst the quantitative analysis utilizes performance metrics.

4.1. Qualitative evaluation of underwater image processing methods using the synthesized images

This section qualitatively analyzes the resultant synthesized images using the selected state-of-the-art enhancement methods and state-of-the-art restoration methods. This analysis is made with the synthesized type-III underwater image as the input image, which is chosen for illustrative purposes.

4.1.1. Qualitative analysis of resultant images from the selected enhancement methods

Fig. 6 shows the enhanced images using the selected enhancement methods, from the type-III synthesized image in Fig. 5(e). It can be seen that the enhancement methods generally produce visually appealing enhanced images. Generally, the enhanced images have high contrast and brightness, and may look visually appealing. However, the enhancement methods may not be able to restore general characteristics of the images as compared to the restoration methods (as shall be discussed further). By using the enhancement method of Zuiderveld [8], the produced image is almost similar to that produced by using restoration methods. By using histogram transformation [7], relative global histogram stretching method [11], and fusion method [30], the resultant images look over enhanced with plenty of noise. On the other hand, the UCM [10] and integrated color model (ICM) [9] enhance the images well without much brightness and contrast, making the enhanced images look appealing.

(a) Image produced by the method of Ancuti et al. [30] (b) Image produced by the method of Hummel [7] (c) Image produced by the method of Iqbal et al. [9]

Fig. 6 Enhanced images using enhancement methods

(d) Image produced by the method of Huang et al. [11]

(e) Image produced by the method of Iqbal et al. [10]

(f) Image produced by the method of Zuiderveld [8]

Fig. 6 Enhanced images using enhancement methods (continued)

4.1.2. *Qualitative analysis of resultant images from the selected restoration algorithms*

As mentioned in previous sections, the original type-III synthesis image is input to the selected state-of-the-art restoration methods. The resultant restored images are given in Fig. 7. It can be seen that, with the method of Yang et al. [18], the image is produced with too much contrast, and hence the image has plenty of noise. With the methods of Carlevaris-Bianco et al. [14], Chao et al. [16], and Song et al. [22], the restored images are relatively cloudy and hazy. A low contrast image is produced by the method of He et al. [15]. Since the restoration method of Li et al. [19] considers only green and blue channels, the restored image looks improperly restored with a reddish tone. With the method of Drews et al. [17], a highly saturated image is produced. On the other hand, with the method of Peng and Cosman [21], the resultant image is identical to the original reference image shown in Fig. 4(a).

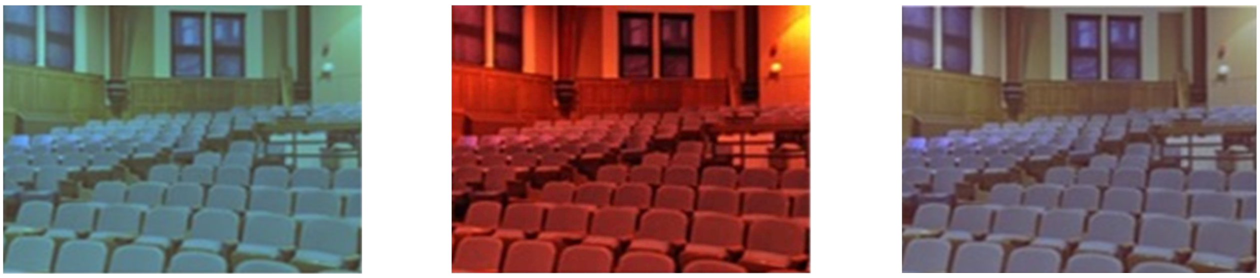

(a) Input image

(b) Image produced by the method of Li et al. [19]

(c) Image produced by the method of Peng et al. [21]

(d) Image produced by the method of Yang et al. [18]

(e) Image produced by the method of Carlevaris-Bianco et al. [14]

(f) Image produced by the method of Chao et al. [16]

(g) Image produced by the method of Drews et al. [17]

(h) Image produced by the method of Song et al. [22]

(i) Image produced by the method of He et al. [15]

Fig. 7 Restored images using restoration methods

4.2. Quantitative evaluation of underwater image processing algorithms using the synthesized images

Quantitative evaluation, using performance metrics, is an important analysis to prove the effectiveness of any method. Both full-reference and non-reference evaluation metrics may be used. PSNR and SSIM may be used for full-reference evaluation, whilst UCIQE [4] and UIQM [5] may be used for non-reference evaluation. PSNR represents the number of errors in the restored image in comparison to the original reference image, whilst SSIM represents the structural similarity between the restored image and the original reference image. Both high PSNR and SSIM values indicate better performance of the enhancement or restoration methods. UCIQE and UIQM are expressed as follows:

$$UCIQE = C_1 \times \sigma_c + C_2 Con_l + C_3 \times \mu_s \tag{3}$$

where C_1= 0.4680, C_2 = 0.2745, and C_3 = 0.2576. σ_c, Con_l, and μ_s are the standard deviations of chroma, the contrast of luminance, and the average saturation of the image [4].

$$UIQM = V_1 \times UICM + V_2 \times UISM + V_3 \times UIConM \tag{4}$$

where V_1 = 0.0282, V_2 = 0.2953, and V_3 = 3.5753. Underwater image colorfulness measure (UICM), underwater image sharpness measure (UISM), underwater image contrast measure (UIConM) are the colorfulness, saturation, and contrast measures of the image [5]. High UCIQE and UIQM values also indicate better performance of the enhancement or restoration methods. These performance metrics are used to quantitatively appraise the selected state-of-the-art enhancement and restoration methods.

4.2.1. Quantitative analysis of resultant images from the selected enhancement methods

Table 2 gives the average PSNR, SSIM, UCIQE, and UIQM values from the enhanced images using different enhancement methods, based on the synthesized images with different water types. The method of Iqbal et al. [9] produces the enhanced images with better PSNR and SSIM scores than other methods because it utilizes ICM in its enhancement process. The PSNR and SSIM values of 11.58 and 0.46, respectively, are obtained [9]. UCM [10], as a modified ICM but concentrates primarily on low-quality images, is also used to produce notable PSNR and SSIM results, albeit lower than the results obtained by the method of Iqbal et al. [9]. The method does not perform well in terms of UCIQE and UIQM, either.

The underwater images enhanced by the method of Ancuti et al. [30] perform well, giving the UCIQE, UIQM, and PSNR values of 0.75, 1.84, and 10.01, respectively. The method of Huang et al. [11] produces good color image metric scores, indicating that the method can enhance the synthesized underwater images well, in terms of the hue, saturation, variance, and chroma of the images. Other methods, however, show comparatively worse performance. Particularly, the methods of Hummel [7] and Zuiderveld [8] do not produce enhanced images with good performance values, and hence, may not be suitable to be used for enhancing underwater images with highly degraded conditions.

Table 2 Quantitative evaluation of underwater enhancement methods

Enhancement method	PSNR ↑	SSIM ↑	UCIQE ↑	UIQM ↑
Zuiderveld et al. [8]	8.71	0.25	0.55	1.49
Hummel et al. [7]	4.82	0.14	0.63	1.50
Iqbal et al. [9]	**11.58**	**0.46**	0.66	1.75
Iqbal et al. [10]	9.70	0.42	0.52	1.42
Huang et al. [11]	9.05	0.31	0.69	1.71
Ancuti et al. [30]	10.01	0.33	**0.75**	**1.84**

*Note: The highest value in each category is highlighted in bold.

4.2.2. *Quantitative analysis of resultant images from the selected restoration algorithms*

Table 3 gives the PSNR, SSIM, UCIQE, and UIQM values from the restored synthesized underwater images using different restoration methods. Both the methods of Peng et al. [21] and Drews et al. [17] produce high metric scores. The former gives the highest PSNR and UCIQE values of 12.70 and 0.89, respectively, among the considered restoration methods, whilst the latter gives the highest SSIM and UIQM values of 0.62 and 1.72, respectively.

These highest values are relatively higher than the highest values obtained from the enhancement methods considered in Table 2, except for the case in which the UIQM value is lower. Other than the method of Peng et al. [21], the methods of Drews et al. [17] and He et al. [15] also produce good PSNR and SSIM values, effectively reducing noise and being capable of restoring structural properties of the image. With regard to the color analysis (i.e., UCIQE and UIQM), the method of Carlevaris-Bianco et al. [14] performs relatively better than other restoration methods, indicating that the color properties of the images can be properly restored, although the method does not perform well in terms of PSNR and SSIM. The method of Song et al. [22] produces average performance in both the full-reference and non-reference metrics. However, other restoration methods do not perform well in this quantitative metric analysis. Recently, Raihan et al. [31] have developed a restoration method of underwater images using depth estimation and attenuation priors, which produces good results for real as well as synthesized underwater images.

Table 3 Quantitative evaluation of underwater restoration algorithms

Restoration method	PSNR ↑	SSIM ↑	UCIQE ↑	UIQM ↑
He et al. [15]	10.15	0.41	0.55	1.45
Li et al. [19]	2.97	0.14	0.19	1.02
Peng and Cosman [21]	**12.70**	0.55	0.89	1.61
Yang et al. [18]	1.21	0.07	0.05	1.18
Carlevaris-Bianco et al. [14]	7.23	0.27	0.65	1.49
Chao et al. [16]	8.45	0.31	0.54	1.51
Drews et al. [17]	11.02	**0.62**	0.58	**1.72**
Song et al. [22]	8.76	0.35	**0.70**	1.43

*Note: The highest value in each category is highlighted in bold.

5. Conclusions

In this study, the generation of underwater images from aerial images has been performed. Due to the conditions of the water medium, underwater images may contain a lot of disturbances, requiring enhancement and restoration before extracting useful information. However, the lack of an underwater dataset and the absence of ground truth reference images are the main challenges for research in this area. The following are the observations from the study.

(1) The process starts with reference images, and hence can be used for performance evaluation of underwater image processing methods.

(2) The test dataset has been developed based on the Jerlov water types, covering all imaging conditions of an underwater environment. For the development process, the background light has been chosen based on the statistical analysis done on a large real underwater image dataset. Attenuation coefficients of 10 water types have been utilized for the design. The synthesis method is efficient and is capable of producing a large synthesized underwater image dataset.

(3) Selected image processing methods have been used to demonstrate the effectiveness of the synthesized dataset, by quantitatively and qualitatively analyzing the output images of the methods.

(4) Enhancement algorithms work well in high turbid conditions, but does not perform well in low turbid images. This is because the enhancement methods focus on the visibility conditions. In contrast, restoration methods focus on structural

characteristics and noise parameters, so they work well only in low turbid conditions and provide reduced visibility characteristics.

(5) The proposed synthesis method can properly evaluate the performance of underwater image processing methods, by providing both synthesized underwater images and their corresponding ground truth images.

The above analysis helps the researchers in this field to choose underwater image processing algorithms that work well in underwater images and paves ways to make improvements for further research purposes. The proposed synthesis method can not only be used to evaluate and improve the underwater image processing methods but also to test the suitability of any computer vision algorithms for different underwater applications.

Conflicts of Interest

The authors declare no conflict of interest.

References

[1] D. W. Jung, S. M. Hong, J. H. Lee, H. J. Cho, H. S. Choi, and M. T. Vu, "A Study on Unmanned Surface Vehicle Combined with Remotely Operated Vehicle System," Proceedings of Engineering and Technology Innovation, vol. 9, pp. 17-24, July 2018.

[2] K. S. Nam, D. G. Lee, J. D. Ryu, and K. N. Ha, "The Basic Study of Underwater Robot Control for Over Actuated Systems," Proceedings of Engineering and Technology Innovation, vol. 12, pp. 21-25, May 2019.

[3] K. Kim and S. Kim, "Cross Layer Based Cooperative Communication Protocol for Improving Network Performance in Underwater Sensor Networks," International Journal of Engineering and Technology Innovation, vol. 10, no. 3, pp. 200-210, June 2020.

[4] M. Yang and A. Sowmya, "An Underwater Color Image Quality Evaluation Metric," IEEE Transactions on Image Processing, vol. 24, no. 12, pp. 6062-6071, October 2015.

[5] K. Panetta, C. Gao, and S. Agaian, "Human-Visual-System-Inspired Underwater Image Quality Measures," IEEE Journal of Oceanic Engineering, vol. 41, no. 3, pp. 541-551, July 2016.

[6] F. F. Koczy and N. G. Jerlov, Photographic Measurements of Daylight in Deep Water, Göteborg: Elanders boktr, 1951.

[7] R. Hummel, "Image Enhancement by Histogram Transformation," Computer Graphics and Image Processing, vol. 6, no. 2, pp. 184-195, April 1977.

[8] K. Zuiderveld, "Contrast Limited Adaptive Histogram Equalization," Graphics Gems IV, pp. 474-485, August 1994.

[9] K. Iqbal, R. A. Salam, A. Osman, and A. Z. Talib, "Underwater Image Enhancement Using an Integrated Colour Model," IAENG International Journal of Computer Science, vol. 34, no. 2, pp. 1-6, November 2007.

[10] K. Iqbal, M. Odetayo, A. James, R. A. Salam, and A. Z. Talib, "Enhancing the Low Quality Images Using Unsupervised Colour Correction Method," IEEE International Conference on Systems, Man, and Cybernetics, pp. 1703-1709, October 2010.

[11] D. Huang, Y. Wang, W. Song, J. Sequeira, and S. Mavromatis, "Shallow-Water Image Enhancement Using Relative Global Histogram Stretching Based on Adaptive Parameter Acquisition," International Conference on Multimedia Modelling, pp. 453-465, February 2018.

[12] A. S. A. Ghani and N. A. M. Isa, "Underwater Image Quality Enhancement through Composition of Dual-Intensity Images and Rayleigh-Stretching," IEEE 4th Conference on Consumer Electronics Berlin, pp. 757- 767, September 2014.

[13] A. J. Raihan, P. E. Abas, and L. C. D. Silva, "Review of Underwater Image Restoration Algorithms," IET Image Processing, vol. 13, no. 10, pp. 1587-1596, June 2019.

[14] N. Carlevaris-Bianco, A. Mohan, and R. M. Eustice, "Initial Results in Underwater Single Image Dehazing," Conference of OCEANS MTS/IEEE Seattle, pp. 1-8, September 2010.

[15] K. He, J. Sun, and X. Tang, "Single Image Haze Removal Using Dark Channel Prior," IEEE Transactions on Pattern Analysis and Machine Intelligence, vol. 33, no. 12, pp. 2341-2353, December 2010.

[16] L. Chao and M. Wang, "Removal of Water Scattering," 2nd International Conference on Computer Engineering and Technology, pp. 1-10, April 2010.

[17] P. Drews, E. Nascimento, F. Moraes, S. Botelho, and M. Campos, "Transmission Estimation in Underwater Single Images," Proc. of IEEE International Conference on Computer Vision Workshops, pp. 825-830, December 2013.

[18] H. Y. Yang, P. Y. Chen, C. C. Huang, Y. Z. Zhuang, and Y. H. Shiau, “Low Complexity Underwater Image Enhancement Based on Dark Channel Prior,” 2nd International Conference on Innovations in Bio-Inspired Computing and Applications, pp. 17-20, December 2011.

[19] C. Li, J. Quo, Y. Pang, S. Chen, and J. Wang, “Single Underwater Image Restoration by Blue-Green Channels Dehazing and Red Channel Correction,” IEEE International Conference on Acoustics, Speech, and Signal Processing, pp. 1731-1735, March 2016.

[20] J. Y. Chiang and Y. C. Chen, “Underwater Image Enhancement by Wavelength Compensation and Dehazing,” IEEE Transactions on Image Processing, vol. 21, no. 4, pp. 1756-1769, April 2012.

[21] Y. T. Peng and P. C. Cosman, “Underwater Image Restoration Based on Image Blurriness and Light Absorption,” IEEE Transactions on Image Processing, vol. 26, no. 4, pp. 1579-1594, April 2017.

[22] W. Song, Y. Wang, D. Huang, and D. Tjondronegoro, “A Rapid Scene Depth Estimation Model Based on Underwater Light Attenuation Prior for Underwater Image Restoration,” 19th Pacific-Rim Conference on Multimedia, pp. 678-688, September 2018.

[23] X. Zhao, T. Jin, and S. Qu, “Deriving Inherent Optical Properties from Background Color and Underwater Image Enhancement,” Ocean Engineering, vol. 94, pp. 163-172, January 2015.

[24] S. Anwar, C. Li, and F. Porikli, “Deep Underwater Image Enhancement,” https://arxiv.org/pdf/1807.03528.pdf, 10 July 2018.

[25] X. Liu and B. M. Chen, “A Systematic Approach to Synthesize Underwater Images Benchmark Dataset and Beyond,” IEEE 15th International Conference on Control and Automation, pp. 1517-1522, July 2019.

[26] C. Li, S. Anwar, and F. Porikli, “Underwater Scene Prior Inspired Deep Underwater Image and Video Enhancement,” Pattern Recognition, vol. 98, 107038, February 2020.

[27] D. Akkaynak, T. Treibitz, T. Shlesinger, R. Tamir, Y. Loya, and D. Iluz, “What Is the Space of Attenuation Coefficients in Underwater Computer Vision?” Proc. of the IEEE Conference on Computer Vision and Pattern Recognition, pp. 4931-4940, November 2017.

[28] M. G. Solonenko and C. D. Mobley, “Inherent Optical Properties of Jerlov Water Types,” Applied Optics, vol. 54, no. 17, pp. 5392-5401, June 2015.

[29] C. Li and X. Zhang, “Underwater Image Restoration Based on Improved Background Light Estimation and Automatic White Balance,” 11th International Conference on Image and Signal Processing, Biomedical Engineering and Informatics (CISP-BMEI), pp. 1-5, October 2018.

[30] C. Ancuti, C. O. Ancuti, T. Haber, and P. Bekaert, “Enhancing Underwater Images and Videos by Fusion,” IEEE Conference on Computer Vision and Pattern Recognition, pp. 81-88, June 2012.

[31] A. J. Raihan, P. E. Abas, and L. C. D. Silva, “ Restoration of Underwater Images Using Depth and Transmission Map Estimation, with Attenuation Priors,” Ocean Systems Engineering, vol. 11, no. 4, pp. 331-351, November 2021.